Supporting Information

Vanadium incorporation induced synergistic enhancement on electron transfer and proton transfer for electrocatalytic benzyl alcohol oxidation

Jingjing Bai,[a] Liang Chen,[a,*] Chenghang Lv,[a] Hongyu Ruo,[a] Yanlong Pan,[a] Shoudong Xu,[b] Jiaqi Chen,[a] Bingchuan Yang,[c,*] Ding Zhang,[d] and Huimin Yang,[a,*]

[a] College of Chemistry, Taiyuan University of Technology, Taiyuan 030024, P. R. China. Email: chenliang@tyut.edu.cn, yanghuimin@tyut.edu.cn

[b] College of Chemical Engineering and Technology, Taiyuan University of Technology, Taiyuan 030024, P. R. China.

[c] College of Chemistry and Chemical Engineering, Qilu Normal University, Jinan 250013, P. R. China. Email: lewis19886@163.com

[d] School of Chemical Engineering and Pharmacy, Wuhan Institute of Technology, Wuhan 430205, P. R. China.

Experimental Section

Materials and Chemicals.

$Ni(NO_3)_2 \cdot 6H_2O$, $Co(NO_3)_2 \cdot 6H_2O$, KOH, VCl_3, and urea were purchased from Sinopharm Chemical Reagent Co., Ltd. Benzyl alcohol, benzaldehyde, benzoic acid, and ethyl acetate were obtained from Aladdin Reagent Co., Ltd. Ethanol and hydrochloric acid (HCl) were purchased from Xilong Chemical Reagent Co. Ltd. Nickel foam (NF) was obtained from Changde Liyuan New Material Co. Ltd. All reagents were of analytical grade and used as received without further purification.

Synthesis of CoV-LDH on nickel foam (CoV-LDH/NF)

Nickel foam (NF) was cleaned to remove the oxide layer on the surface. First, it underwent a 20-min ultrasonic cleaning soaking in 1 M HCl. Subsequently, it was ultrasonicated separately with deionized (DI) water and alcohol for 20 min. Afterward, it was dried in a vacuum oven at 70 °C for 6 h. The CoV-LDH/NF composite was prepared via a hydrothermal method. Specifically, 0.349 g of $Co(NO_3)_2 \cdot 6H_2O$ and 0.063 g of VCl_3 were dissolved in 40 mL DI water. Then, 0.3 g of urea was added with continuous stirring. The resulting solution was transferred to a 50 mL Teflon-lined stainless-steel autoclave. A piece of cleaned NF (2×5 cm^2) was placed in the autoclave, which was sealed and maintained at 120 °C for 12 h. After naturally cooling to room temperature, the CoV-LDH/NF composite was rinsed with DI water and ethanol before

being dried in a vacuum oven at 50 °C for 6 h. For the preparation of $Co(OH)_2$/NF, the same method was used, except that VCl_3 was not added.

Synthesis of CoNi-LDH on nickel foam (CoNi-LDH/NF)

A one-step hydrothermal method was used to separate 0.349 g $Co(NO_3)_2 \cdot 6H_2O$ and 0.116 g $Ni(NO_3)_2 \cdot 6H_2O$ were dissolved into 40 mL of deionized water by one-step hydrothermal method, after which 0.3 g of urea was added and transferred to a 50 mL reactor with sufficient stirring to fully immerse the nickel foam. Finally, the reaction kettle was placed in an oven and reacted at 120 ℃ for 12 h. After the reaction was completed and cooled naturally, the nickel foam in the reaction kettle was removed, the remaining solution was filtered, and washed with deionized water and ethanol for several times, respectively. The nickel foam and powder were then dried in a vacuum oven at 70 ℃ for 6 h to obtain CoNi-LDH/NF and CoNi-LDH powder loaded on nickel foam.

Material characterization

Powder X-ray diffraction (XRD) analysis was conducted using a Bruker D8 Advance powder diffractometer equipped with Cu K_α X-ray radiation (λ = 1.5406 Å). Scanning electron microscopy (SEM) images were acquired by FEI Talos-S. Transmission electron microscopy (TEM) was performed by JEOL JSM-7100F operated at 200 kV. X-ray photoelectron spectroscopy (XPS) spectra were collected using a Thermo ESCALAB 250Xi X-ray photoelectron spectrometer. The shift of the binding energy

was corrected using C 1*s* as an internal standard at 284.8 eV. Raman spectra were obtained with a Renishaw micro-Raman spectrometer via a laser (532 nm) as the exciting source. Ultraviolet Photoelectron Spectrometer (UPS) was performed by Thermofisher ESCALAB 250Xi carried out with a helium discharge lamp (hv = 21.22 eV) in normal emission with a sample bias of −10 V. The UV-vis diffuse reflection spectra (DRS) were recorded on a Hitachi UH-4150 spectrophotometer equipped with an integrated sphere attachment, with $BaSO_4$ serving as the reference. The bandgap widths of the catalysts were determined using the formula $(\alpha hv)^{1/n}=A(hv-E_g)$, where α is the absorption index, h is the Planck constant, v denotes the frequency, A is a constant, and E_g represents the bandgap width of semiconductor. The pH of electrolyte was measured by a PHSJ-5 pH meter manufactured by Leici, Co. Ltd., China. The Inductively Coupled Plasma Optical Emission Spectrometry (ICP-OES) used is an Agilent 5110 of America for the test, and the liquid to be tested was treated with acid solution for the test.

Electrochemical measurements

Electrochemical measurements were conducted using a Corrtest CS3104 electrochemical workstation with a three-electrode system, in which graphite rod and Hg/HgO electrode were selected as the counter electrode and reference electrode, respectively. The as-prepared catalyst served as the working electrode. The applied potential was calibrated

based on the reversible hydrogen electrode (RHE), using the equation of E (*vs*. RHE) = E (*vs*. Hg/HgO) + 0.098 V + 0.059 V × pH. The current density was normalized to the geometric area of the working electrode (1×1 cm^2). The oxygen evolution reaction (OER) and benzyl alcohol oxidation reaction (BOR) experiments were performed in separate 30 mL solutions: 1 M KOH and 1 M KOH with 0.1 M benzyl alcohol, respectively. Prior to the electrochemical measurement, 20 cycles of cyclic voltammetry (CV) were conducted at scan rate of 50 mV s^{-1} in the range of 0~0.6 V (*vs*. Hg/HgO) to stabilize the catalyst. To evaluate the electrochemical performance of the catalysts, CV was performed at a scan rate of 5 mV s^{-1} in a potential window of 0~0.6 V (*vs*. Hg/HgO), selecting the reduced branch curve and correcting with manual 90% *iR*. The electrochemical surface area (ECSA) was determined through CV scans conducted within a potential range of 1.11~1.21 V (*vs*. RHE) with scanning rates ranged from 20 to 100 mV s^{-1}. The ECSA was calculated using the formula ECSA = C_{dl}/C_s, where C_{dl} and C_s correspond to the double layer capacitance and specific capacitance, respectively. The C_{dl} value can be evaluated by analyzing the slope between $\Delta j/2$ at 1.16 V (*vs*. RHE) and the scan rate. And C_s can be determined based on the scanning rate and the integral of $\frac{\int_{V_1}^{V_2} I\,dV}{2\Delta V}$.

Mott-Schottky (M-S) plots were obtained in the aforementioned three-electrode system at AC frequency of 3, 4, and 5 kHz. Conversion of RHE to NHE scale, we utilized the Nernst equation:

$$E\ (vs.\ \text{RHE}) = E\ (vs.\ \text{NHE}) + 0.059\ \text{V} \times \text{pH}$$

Operando electrochemical impedance spectroscopy (EIS) was carried out at a potential range of 0~0.8 V (*vs*. Hg/HgO), with a frequency ranging from 0.1 Hz to 100 kHz and an amplitude of 5 mV.

Product analysis

The products of the oxidation reaction of benzyl alcohol were analyzed by gas chromatography (GC, Shanghai haixin GC-950) equipped with a flame ionization detector. Initially, the electrocatalytic BOR was carried out at a constant potential of 1.44 V (*vs*. RHE). The resulting products were extracted with ethyl acetate and then analyzed by GC.

3 M HCl was added into the electrolyte after the EBA reaction to achieve the conversion from Ph-COOK to Ph-COOH. Then, the Ph-COOH crystal containing KCl was separated by suction filtration from the electrolyte, and dried at 60 ℃ for 30 min.

The Coversion(%), yield(%) and reaction selectivity(%) of benzoic acid formation were calculated as follows:

$$\text{Coversion} = \frac{n(\text{reacted benzyl alcohol})}{n(\text{intial benzyl alcohol})} \times 100\%$$

$$\text{Selectivity} = \frac{n(\text{benzoic acid production})}{n(\text{reacted benzyl alcohol})} \times 100\%$$

$$\text{Yield} = \frac{n(\text{benzoic acid production})}{n(\text{intial benzyl alcohol})} \times 100\%$$

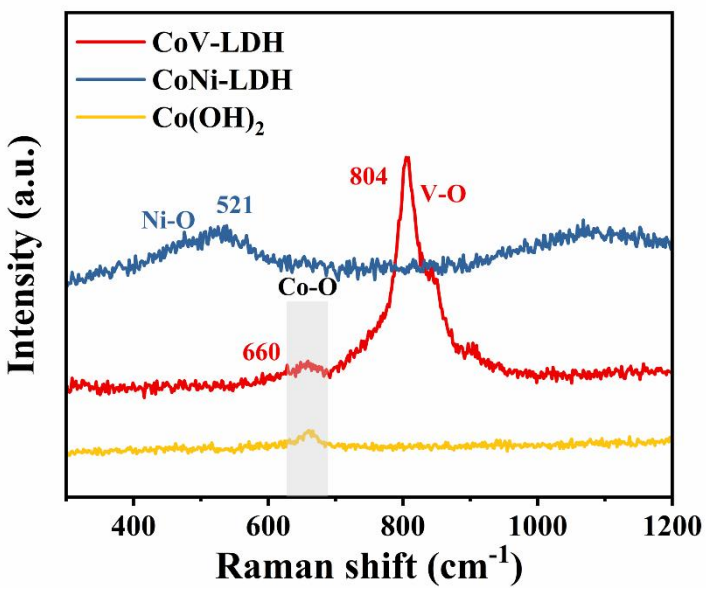

Figure S1. Raman spectra of CoV-LDH/NF, CoNi-LDH/NF and $Co(OH)_2$/NF.

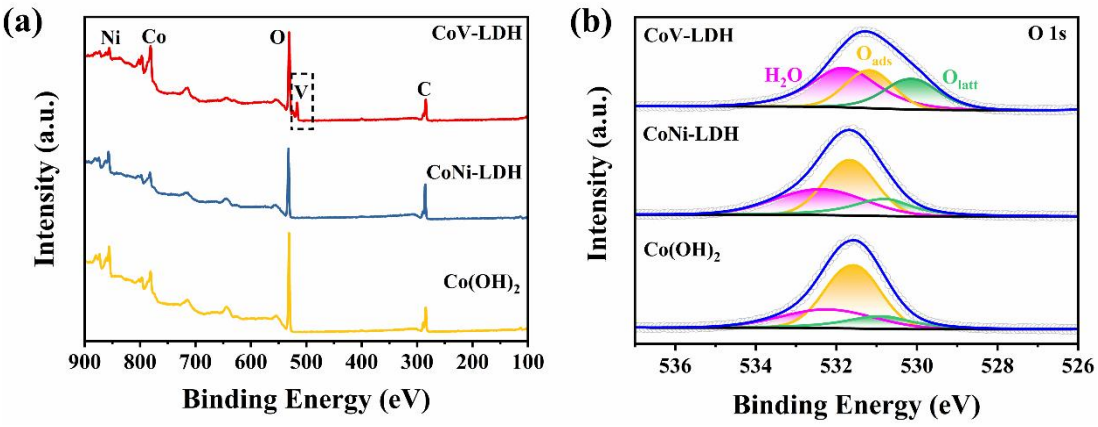

Figure S2. XPS spectra for CoV-LDH/NF and the controlled samples: (a) survey and (b) high-resolution spectra of O 1*s*.

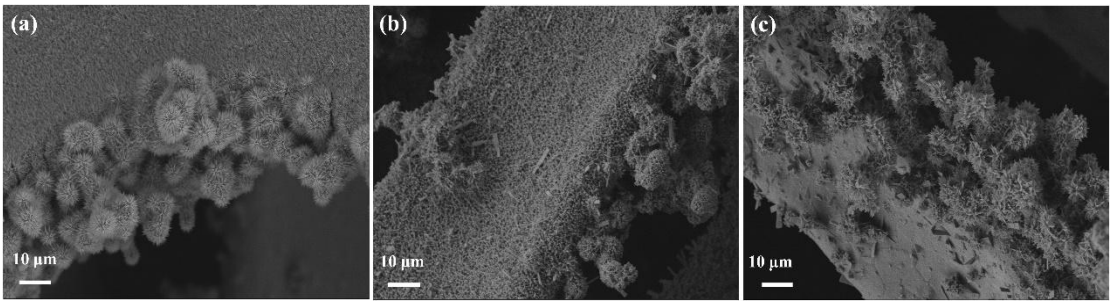

Figure S3. Low magnification SEM images of (a) CoV-LDH/NF, (b) CoNi-LDH/NF, and (c) $Co(OH)_2$/NF.

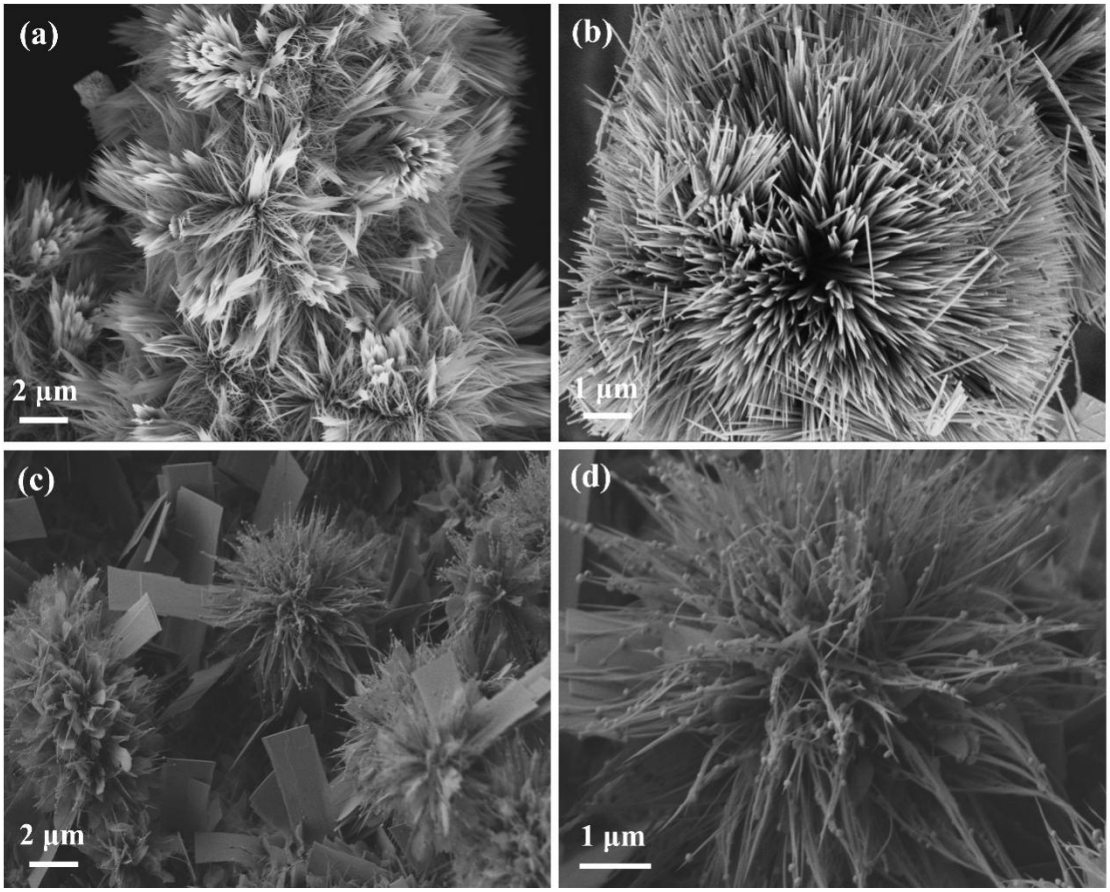

Figure S4. SEM images of (a-b) CoNi-LDH and (c-d) $Co(OH)_2$.

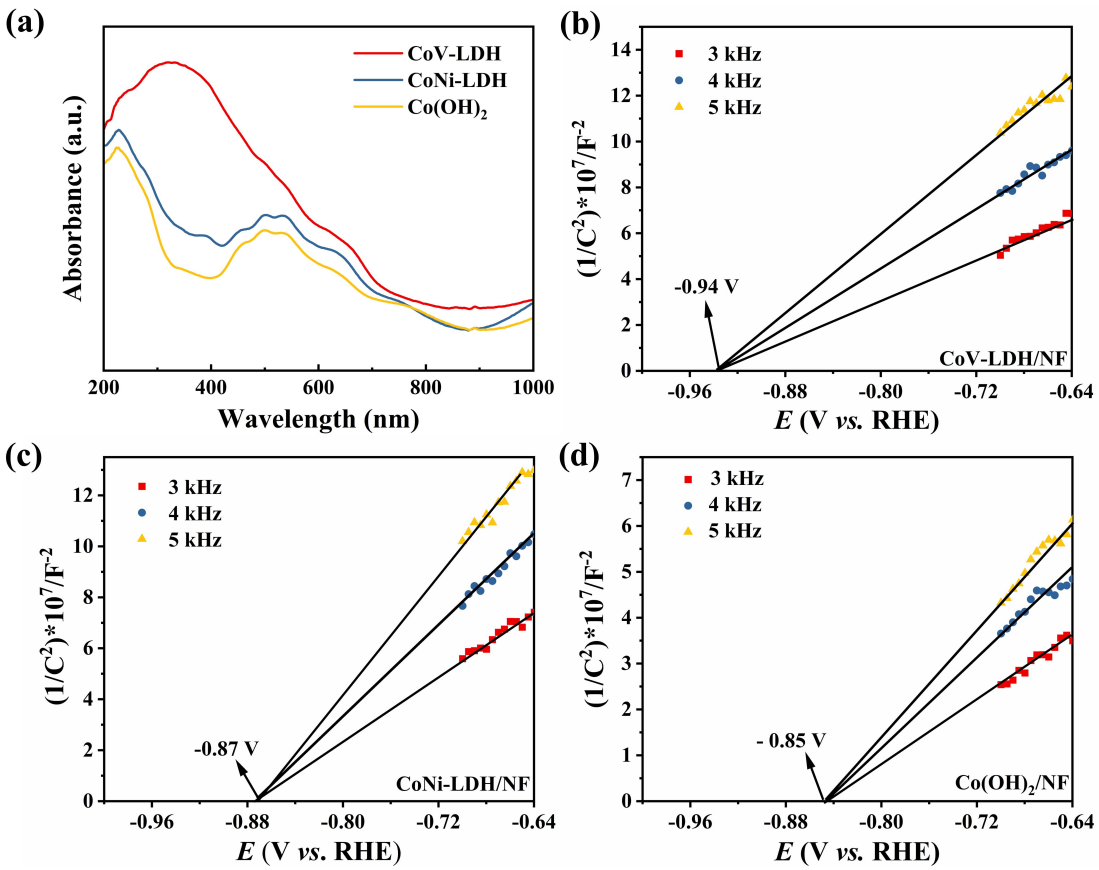

Figure S5. (a) UV-vis diffuse reflectance spectra, Mott-Schottky plots of (b) CoV-LDH/NF, (c) CoNi-LDH/NF, and (d) $Co(OH)_2$/NF.

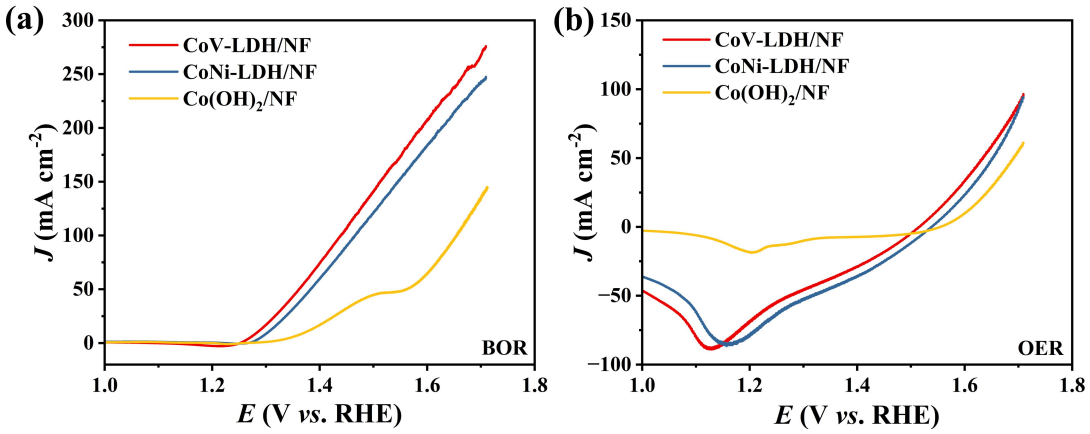

Figure S6. Polarization curves of the three samples for BOR and OER without 90 % *iR* compensation.

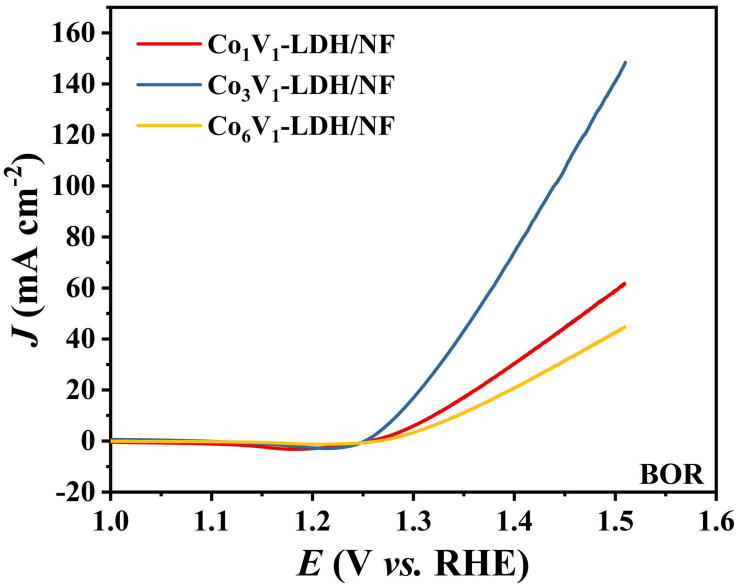

Figure S7. LSV curves of Co_xV_y-LDH electrocatalysts for BOR.

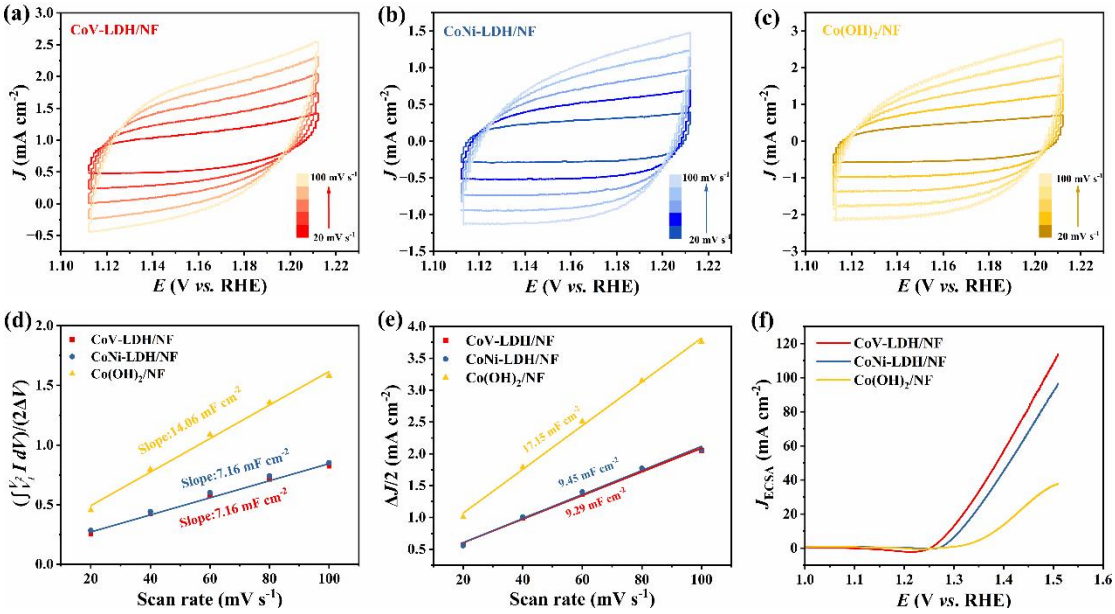

Figure S8. CVs at different scan rates from 20 mV s^{-1} to 100 mV s^{-1} conducted on (a) CoV-LDH/NF, (b) CoNi-LDH/NF, and (c) $Co(OH)_2$/NF. (d) Calculation of *C*s: Plots of scan rate (v) and $\int_{V_1}^{V_2} I\,\mathrm{d}V/2\Delta V$. (e) Double layer charging current density ($\Delta J/2$) plotted against scan rate. (f) ESCA normalized BOR activity.

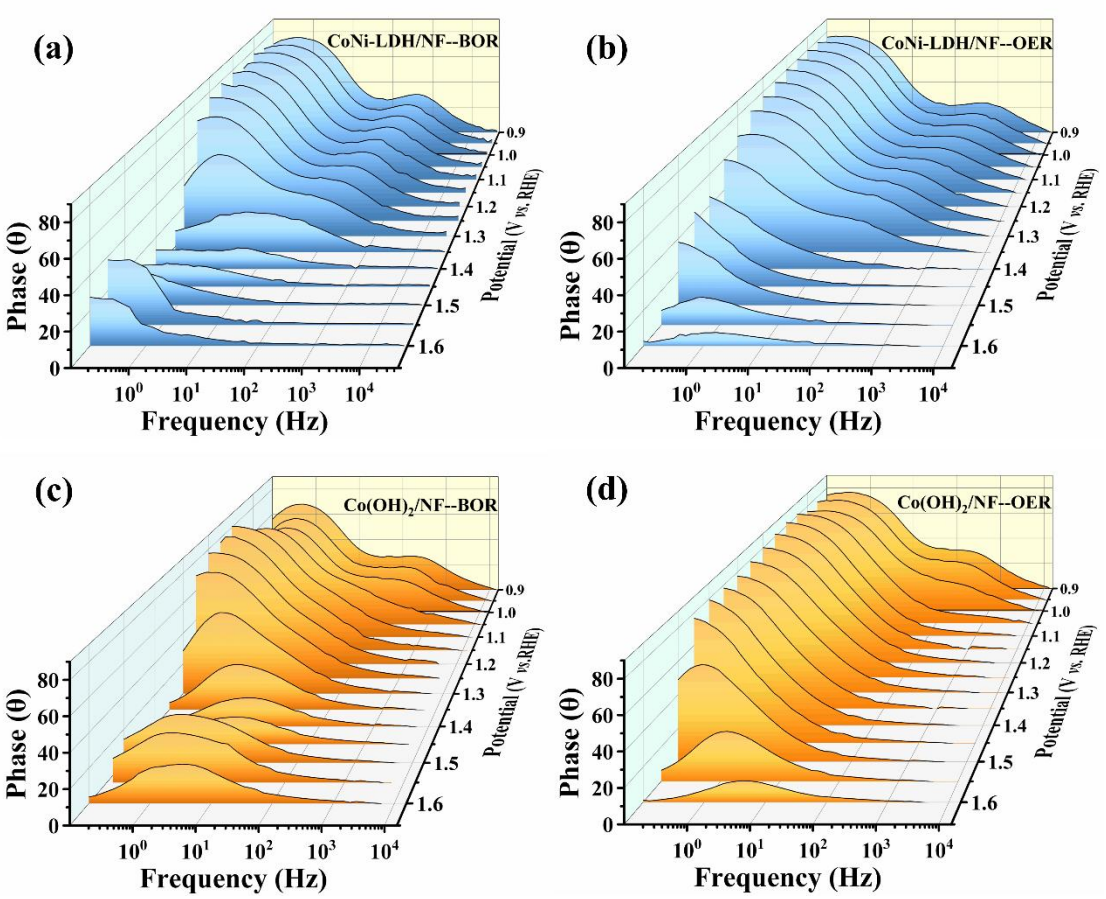

Figure S9. Under different potentials using Operando EIS analysis. (a, b) CoNi-LDH/NF and (c, d) $Co(OH)_2$/NF.

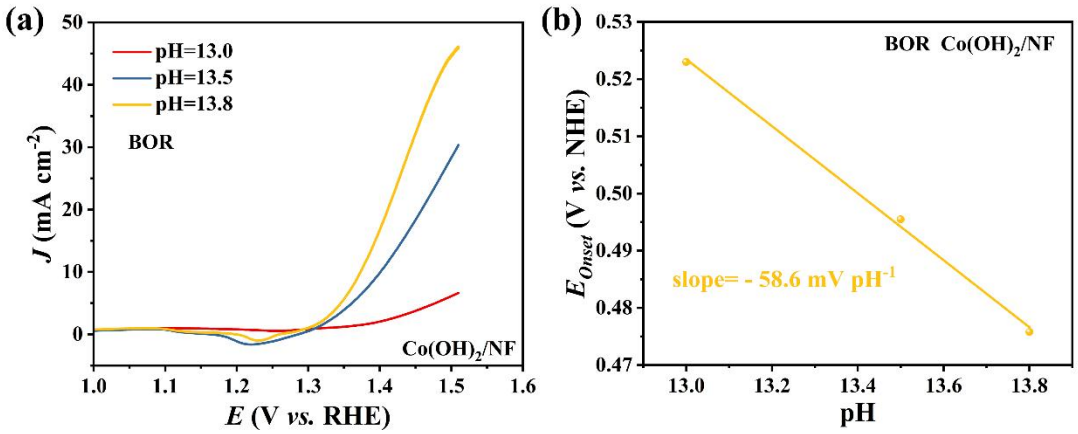

Figure S10. (a) LSV curves of $Co(OH)_2$/NF in KOH solutions with 0.1 M benzyl alcohol as a function of pH and (b) the effect of pH on the onset potential.

Table S1. Comparison of the catalytic performance of the CoV-LDH/NF and other catalysts towards benzyl alcohol electrochemical oxidation in 1.0 M KOH.

Electrocatalyst	Electrolyte	Potential@Current density density (V vs. RHE @ mA cm^{-2})	Ref.
hp-Ni	0.01 M BA	>1.35@10	[S1]
Fe/Co200	0.015 M BA	1.42@10	[S2]
NiCo/AC	0.1 M BA	1.31@10	[S3]
Mo-Ni/MoO_2/Ni	0.1 M BA	1.35@15	[S4]
MoO_2-FeP	0.01 M BA	>1.37@20	[S5]
Ni-MOF@CNT	0.5 M BA	>1.4@25	[S6]
Ni-OH/NF	0.1 M BA	1.33@100	[S7]
CuO-NRs	0.01 M BA	>1.4@10	[S8]
Ni-2D-O-SA-CNT	0.1 M BA	1.51@77	[S9]
NiO/Ni_3S_2	0.2 M BA	1.391@50	[S10]
CF-220	0.05 M BA	1.4@10	[S11]
Au_{1+n}-NiAl-LDH	0.01 M BA	1.455@1	[S12]
NiOOH	0.1 M BA	1.36@10	[S13]
$NiCo(OOH)_x$	0.1 M BA	1.35@50	[S14]
Au/CoOOH	0.1 M BA	1.5@540	[S15]
CoV-LDH/NF	0.1 M BA	1.28@10 1.31@100	This work

Table S2. The elemental analysis data for Co_xV_y-LDH from ICP-OES results

Samples	Feed ratio of Co:V	Content of Co W (%)	Content of V W (%)	Measured ratio (Co:V)
CoV-LDH	1:1	27.67	21.20	1.3:1
Co_3V_1-LDH	3:1	40.02	12.16	3.3:1
Co_6V_1-LDH	6:1	47.16	7.38	6.4:1

Reference

[S1] B. You, X. Liu, and Y. Sun, Efficient H_2 Evolution Couple with Oxidative Refining of Alcohols via A Hierarchically Porous Nickel Bifunctional Electrocatalysis, *ACS Catalysis*, 2017, **7**, 4564-4570.

[S2] Y. Huang, R. Yang, G. Anandhababu, J. Xie, J. Lv, X. Zhao, X. Wang, M. Wu, Q. Li and Y. Wang, Cobalt/Iron(Oxides) Heterostructures for Efficient Oxygen Evolution and Benzyl Alcohol Oxidation Reactions, *ACS Energy Lett.,* 2018, **3**, 1854−1860.

[S3] G. Liu, C. Zhao, G. Wang, Y. Zhang and H. Zhang, Efficiently electrocatalytic oxidation of benzyl alcohol for energy-saved zinc-air battery using a multifunctional nickel-cobalt alloy electrocatalyst, *J. Colloid Interface Sci.*, 2018, **532**, 37-46.

[S4] X. Cui, M. Chen, R. Xiong, J. Sun, X. Liu and B. Geng, Ultrastable and efficient H_2 production via membrane-free hybrid water electrolysis over a bifunctional catalyst of hierarchical Mo-Ni alloy nanoparticles, *J. Mater. Chem. A*, 2019, **7**, 16501-16507.

[S5] G. Yang, Y. Jiao, H. Yan, Y. Xie, A. Wu, X. Dong, D. Guo, C. Tian and H. Fu, Interfacial Engineering of MoO_2-FeP Heterojunction for Highly Efficient Hydrogen Evolution Couple witn Biomass Electrooxidation, *Adv. Mater.*, 2020, **32**, 2000455.

[S6] T. V. M. Sreekanth, G. R. Dillip, P. C. Nagajyothi, K. Yoo and J. Kim, Integration of Marigold 3D flower-like Ni-MOF self-assembled on MWCNTs via microwave irradiation for high-performance electrocatalytic alcohol oxidation and oxygen evolution reactions, *Applied Catalysis B: Environmental*, 2021, **285**, 119793.

[S7] L. Ming, X. Wu, S. Wang, W. Wu and C. Lu, Facile growth of transition metal hydroxide nanosheets on porous nickel foam for efficient electrooxidation of benzyl alcohol, *Green Chem.,* 2021, **23**, 7825-7830.

[S8] Z. Fang, P. Zhang, M. Wang, F. Li, X. Wu, K. Fan and L. Sun, Selective Electro-oxidation of Alcohols to the Corresponding Aldehydes in Aqueous Solution via Cu(III) Intermediates from CuO Nanorods, *ACS Sustainable Chem. & Eng.*, 2021, **9**, 11855-11861.

[S9] Z. Liang, D. Jiang, X. Wang, M. Shakouri, T. Zhang, Z. Li, P. Tang, J. Llorca, L. Liu, Y. Yuan, M. Heggen, R. E. Dunin-Borkowski, J. R. Morante, A. Cabot and J. Arbiol, Molecular Engineering to Tune the Ligand Environment of Atomically Dispersed Nickel for Efficient Alcohol Electrochemical Oxidation, *Adv. Funct. Mater.,* 2021, **31**, 2106349.

[S10] R. Li, P. Kuang, L. Wang, H. Tang and J. Yu, Engineering 2D NiO/Ni_3S_2 heterointerface electrocatalyst for highly efficient hydrogen production coupled with benzyl alcohol oxidation, *Chemical Engineering Journal*, 2022, **431**, 134137.

[S11] Y. Han, C. Yu, H. Huang, Q. Wei, J. Dong, L. Chen and J. Qiu, Controllable surface reconstruction of copper foam for electrooxidation of benzyl alcohol integrated with pure hydrogen production, *SmartMat.,* 2024; **5**, e1206.

[S12] Z. Song, T. Shen, Y. Hu, G. Liu, S. Bai, X. Sun, S. M. Xu and Y. F. Song, Coexistence of Au single atoms and Au nanoparticles on NiAl-LDH for selective electrooxidation of benzyl alcohol to benzaldehyde, *Nanoscale*, 2023, **15**, 11867-11874.

[S13] Y. Hao, J. Li, X. Cao, L. Meng, J. Wu, X. Yang, Y. Li, Z. Liu and M. Gong, Origin of the Universal Potential-Dependent Organic Oxidation on Nickel Oxyhydroxide, *ACS Catal*. 2023, **13**, 5, 2916-2927.

[S14] M. Zhang, Zh. Xu, B. Liu, Y. Duan, Z. Zheng, L. Li, Q. Zhou, V. G. Matveeva, Z. Hu, J. Yu and K. Yan, Anchoring hydroxyl intermediate on NiCo$(OOH)_x$ nanosheets to enable highly efficient electrooxidation of benzyl alcohols, *AIChE J.*, 2023, **69**, e18077.

[S15] Z. Li, Y. Yan, S. M. Xu, H. Zhou, M. Xu, L. Ma, M. Shao, X. Kong, B. Wang, L. Zheng and H. Duan, Alcohols electrooxidation coupled with H_2 production at high current densities promoted by a cooperative catalyst, *Nat Commun.*, 2022, **13**, 147.